MODELING OF DAMAGE BEHAVIOR OF AN ENVIRONMENTAL BARRIER COATED CERAMIC MATRIX COMPOSITE UNDER THERMAL LOADINGS

Thomas Vandellos[1], Edouard Thebaud[1] and Thibaut Archer[2]

[1] Safran Ceramics, a technology platform of Safran Tech, Le Haillan, France,
thomas.vandellos@safrangroup.com, Edouard.thebaud@safrangroup.com,
https://www.safran-group.com

[2] DMAS, ONERA The French Aerospace Lab, Châtillon, France, Thibaut.archer@onera.fr,
https://www.onera.fr

Keywords: Ceramic matrix composite, environmental barrier coating, thermal gradient, damage model

ABSTRACT

Development of structures with environmental barrier coated ceramic matrix composite materials requires a perfect understanding of the behavior and the damage mechanisms of CMC/EBC system under loadings close to turbine engines applications. Firstly, this article describes thermal gradient tests realized with a high heat flux laser multi-instrumented by an infrared camera, visible light cameras, acoustic emission sensors and a bichromatic pyrometer. In order to avoid differences between experimental and numerical data, the computed temperature field is identified using a Finite Element Model Updating method on the laser beam shape. Finally, thermomechanical simulation of the test is conducted considering a damage model describing the CMC behavior. Discussions are proposed about the localization of the damage area predicted by the model, compared to the cracks experimentally observed, and about the influence of the choice for modeling the coating behavior.

1 INTRODUCTION

SiC/SiC Ceramic Matrix Composites (CMC) represent an interesting alternative to metallic materials, particularly for the development of turbine parts of aircraft engines, thanks to their good properties at high temperature (until 1300°C) and their low density [1, 2]. However, SiC-based CMCs need to be protected by an environmental barrier coating (EBC) to avoid the surface recession phenomenon because of the presence of water vapor under typical service environments [3]. Thus, the design of CMC structures implies to justify the adhesion of the coating on the CMC substrate and to understand the behavior and the damage mechanisms of the CMC/EBC system under complex thermomechanical loadings [4-6]. This article focuses on the system behavior under thermal gradient loadings using three key points (Fig. 1):

- to perform characterization tests under thermal gradients using a multi-instrumented high heat flux CO_2 laser setup, available at ONERA,
- to implement a finite element model whose thermal boundary conditions are identified using measured thermal fields and
- to model the experimental tests taking into account nonlinear behavior of the materials.

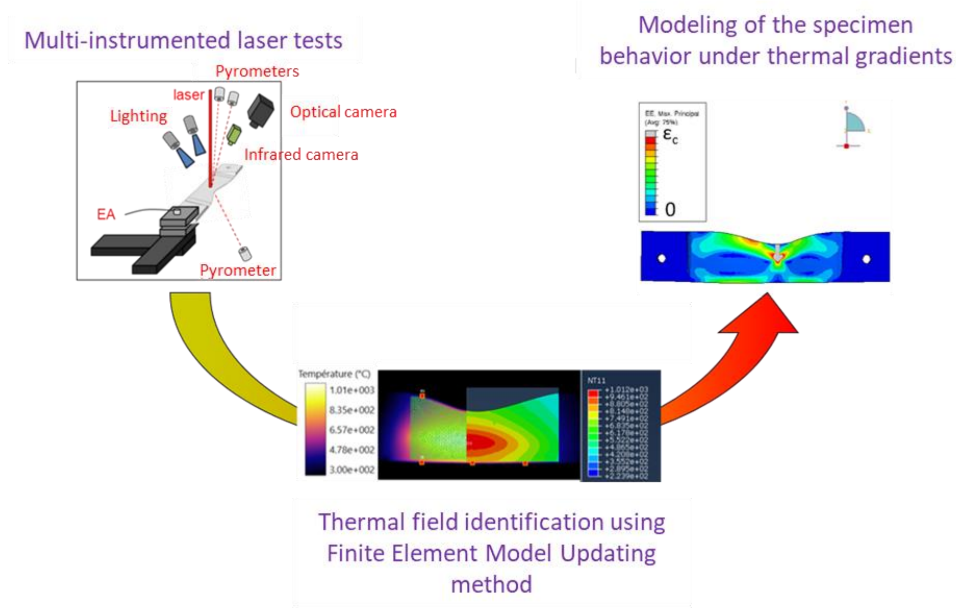

Figure 1: Illustration of the three key steps for characterizing and modeling the CMC/EBC behavior under thermal gradient loadings.

2 MULTI-INSTRUMENTED LASER TESTS ON CMC/EBC SPECIMENS

Thermomechanical tests were performed with a high heat flux CO_2 laser setup, available at ONERA, on a 3D woven ceramic matrix composite material named CERASEP®A600 coated by a thin layer of ytterbium disilicate (<100µm). A silicon bond coat ensures the adhesion of the top coat on the CMC substrate. Its thickness was comparable to the thickness of the rare earth layer. In this study, the specimen had geometric specificities with a variable thickness of the CMC material from 2mm to 0.2mm and a curvature shape where the thickness is thinner.

In order to measure and control the applied thermal boundary conditions during thermomechanical tests, infrared cameras and bichromatic pyrometers were set up. Moreover, visible light cameras and acoustic emission sensors were used to analyze the material behavior and detect damage onset and accumulation during the test. Fig. 2 shows the multi-instrumented laser setup, the shape of the tested specimen and an example of thermal field inducing by the laser heating.

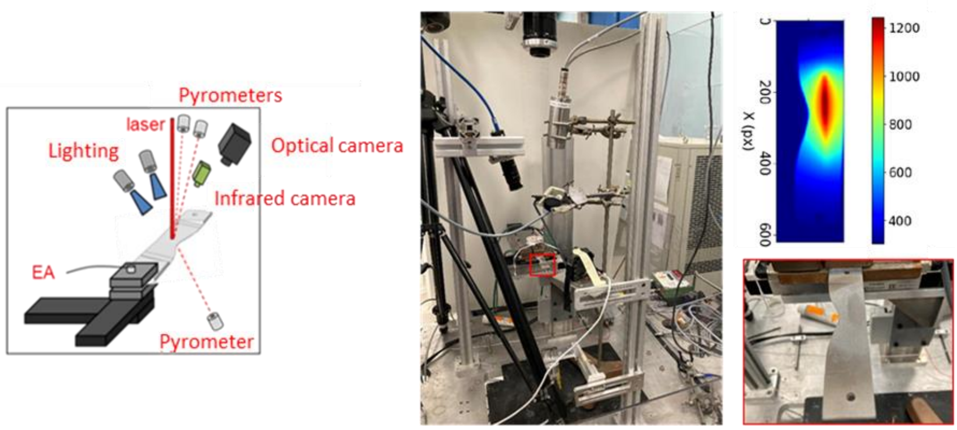

Figure 2: Schematic description and photos of the multi-instrumented laser setup, photo of the specimen and picture of the thermal field with thermal gradient.

Two kinds of thermomechanical tests were carried out. The first one was a fatigue thermal test with 30 cycles. A single thermal cycle is described with 1 minute of rise time, a 10 minutes stabilized heating stage and a cooling stage of 1 minute. The maximum temperature was under the laser spot at the surface of the top coat. This temperature, measured by the infrared camera and the bichromatic pyrometer, was equal to 800°C for the first 10 cycles, 1050°C for the next 10 cycles and 1250°C for the last 10 cycles. As shown on Fig. 3a with the normalized cumulative acoustic energy, few signals are detected during the cycles at 800°C. Next, for the cycles at 1050°C, acoustic emission activates particularly during the heating stage of the first cycle. Finally, for the last cycles at 1250°C (under the laser spot), the normalized cumulative energy increases at each heating stage, indicating probably the cracking onset and the damage growth into the CMC material.

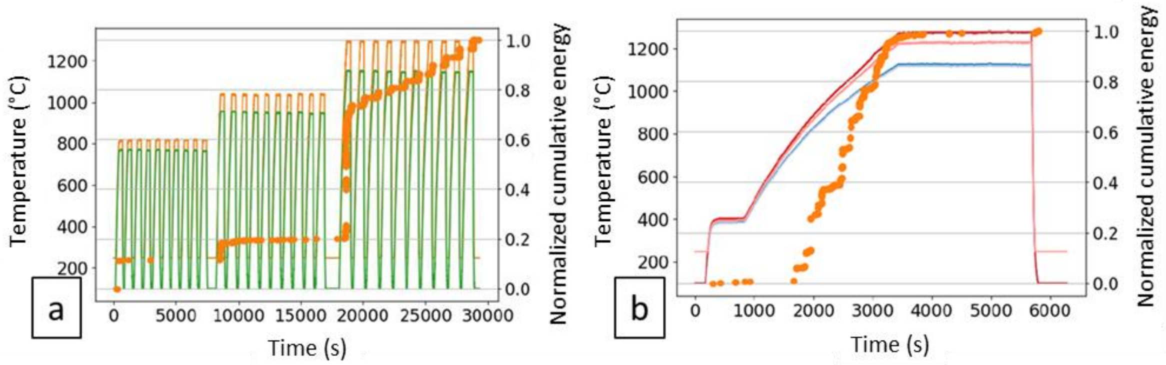

Figure 3: Evolution of maximum temperature as function of time (a) during a thermal cyclic test with three levels of temperature and (b) during a thermal monotonic loading.

From these results, a second thermomechanical test was performed with a monotonic loading from room temperature to 1250°C (under the laser spot), as illustrated on Fig. 3b. As previously, acoustic emission signals start when the temperature reaches 800°C and the normalized cumulative acoustic energy becomes higher when the maximum temperature overcome 1000°C.

To identify the damage mechanisms occurring at the end of the tests, scanning electron microscope (SEM) observations were realized and a crack through the thickness of the CMC/EBC system was detected at the middle of the specimen. Its length was close to the half of the width and its opening was inferior to 11µm (Fig. 4).

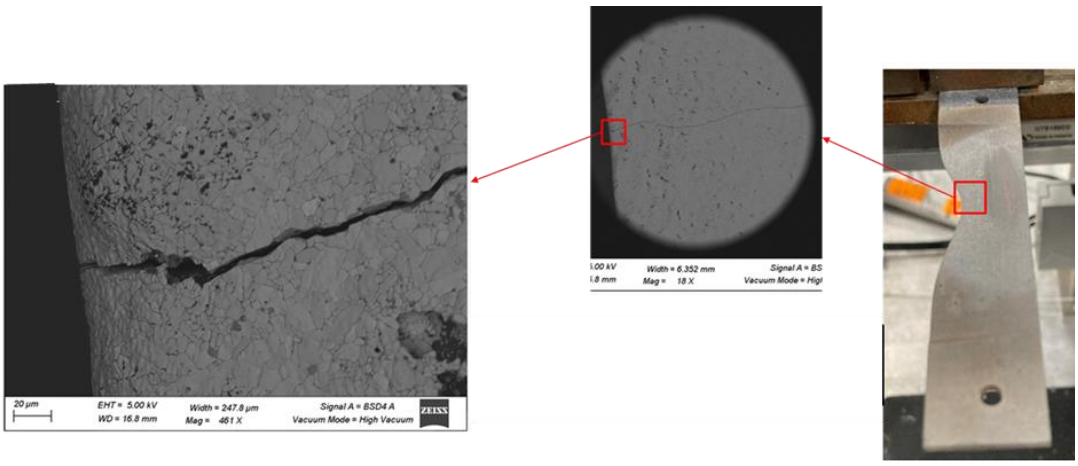

Figure 4: Crack detected by Scanning Electron Microscopy (SEM) observation and its localization on the specimen.

In order to understand how this type of failure appears during the thermal loading, a modeling of the thermal monotonic test was realized.

3 ESTABLISHMENT OF THE MODEL WITH TEMPERATURE FIELD IDENTIFICATION USING FINITE ELEMENT MODEL UPDATING METHOD

In this work, the understanding of the behavior and the damage mechanisms of the system under laser heating requires finite element simulations closed to the experimental conditions. To obtain a good correlation between computed and measured thermal fields, the following steps were realized:

- the establishment of a reference model for which the thermal fields, measured by the infrared camera on the top surface of the specimen, were applied as boundary conditions. The purpose of this step was only to project the measured thermal fields on the mesh of the finite element model. The software Eikotwin DIC allows this projection (Fig. 5) using selection of some characteristic points of the specimen's geometry.

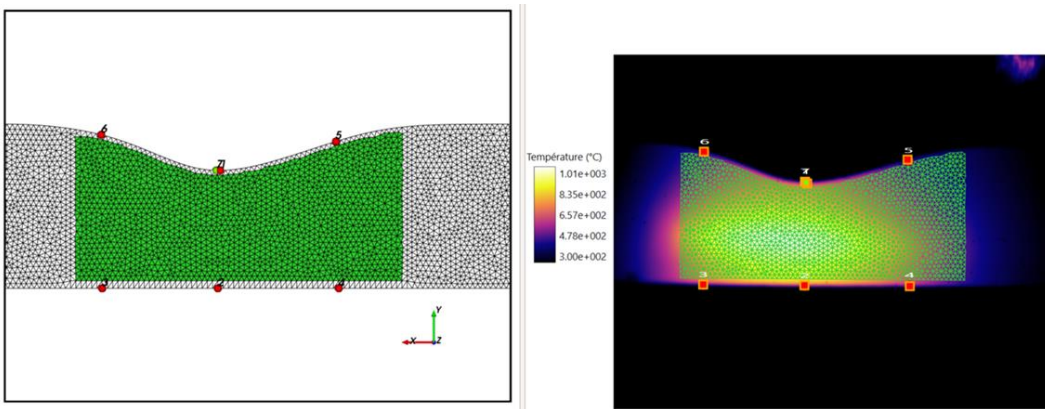

Figure 5: Mesh projection on the thermal field, measured by infrared camera, by the Eikotwin software.

- the use of a finite element model with, as boundary conditions, (i) a thermal flux on the heated surface (illustrated on Fig. 6), representing the laser heating on the top surface, and (ii) convection and radiative heat transfers on the others surfaces of the specimen. The thermal flux Φ was defined using the Eq. 1 where A corresponds to the flux magnitude, X0 and Y0 the coordinates of the laser center, ζ_x the laser width in X-direction, ζ_y the laser width in Y-direction, η_x the Gaussian parameter for X-direction and η_y the Gaussian parameter for Y-direction.

$$\Phi = Ae^{\frac{|Y-Y_0|^{\eta_y}}{\zeta_y} - \frac{|X-X_0|^{\eta_x}}{\zeta_x}} \tag{1}$$

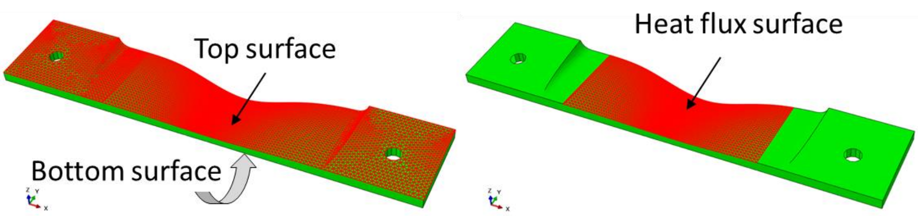

Figure 6: Surfaces used for thermal conditions.

- the identification of the laser shape using Finite Element Model Updating (FEMU) on the temperature fields. This method allows the identification of the parameters using an iterative loop minimizing the difference between the computed thermal field and the reference thermal field (obtained by the first model). The Fig. 7 shows the comparison between the measured and the computed thermal fields.

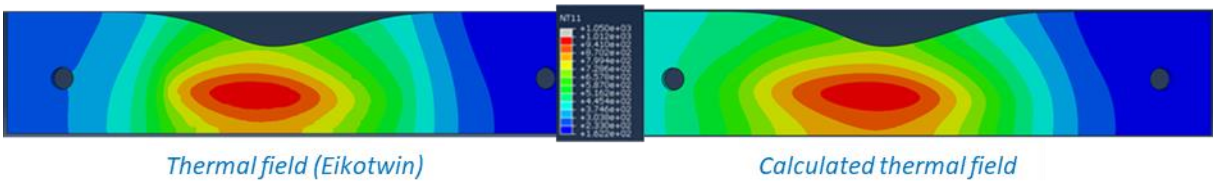

Figure 7: Comparison between the measured (projected on the mesh) and the computed thermal fields.

Using this model where the thermal boundary conditions were identified, it was possible to study the thermomechanical behavior of the CMC/EBC system.

4 MODELING OF THE COATED CMC SPECIMEN BEHAVIOR UNDER THERMAL GRADIENT LOADINGS

4.1 Modeling of the CMC material under thermal gradient

Firstly, the simulation of the experimental test was performed neglecting the coating. Thus, only the CMC material was described in the finite element model. This material has transversally isotropic elastic properties (the longitudinal orientation in length direction and the transverse orientation in width direction) and, after the elastic domain, had a damage behavior induced by the progressive accumulation of matrix cracking and of the yarn failure. Thus, two kinds of modeling were realized:

- the first one with an elastic behavior. With this model, Fig. 8a indicates (i) that the principal max strain overcomes the elastic strain threshold ε_0 (grey area on the picture corresponding to the damaged volume) at the free edge of the specimen when the temperature reaches 800°C under the laser spot, and (ii) that this damaged area growths progressively with the heating stage. At the end of the loading, the damaged area presents an oval shape where the width and the length attain the quarter of the specimen dimensions. It is important to note that the difference of thermal expansion of the material, due to the thermal gradient, explains the stress state responsible of the damaged area. This stress state is exacerbated by the thin thickness on one side of the specimen.
- The second one with a damage model, named ONERA Damage Model (ODM) [7], to describe the nonlinear behavior induced by the progressive accumulation of damages in the CMC material. Fig. 8b shows, as the previous model, an overcoming of the elastic threshold from a temperature of 800°C under the laser spot. However, with the heating stage, the damaged area decreases in the length direction but growths in the width direction from the quarter to the middle of the specimen. This observation can be explained by the yarn failures of the CMC material which promote the local load transfer. The yarn failure predicted and its localization correlate with the critical failure experimentally observed.

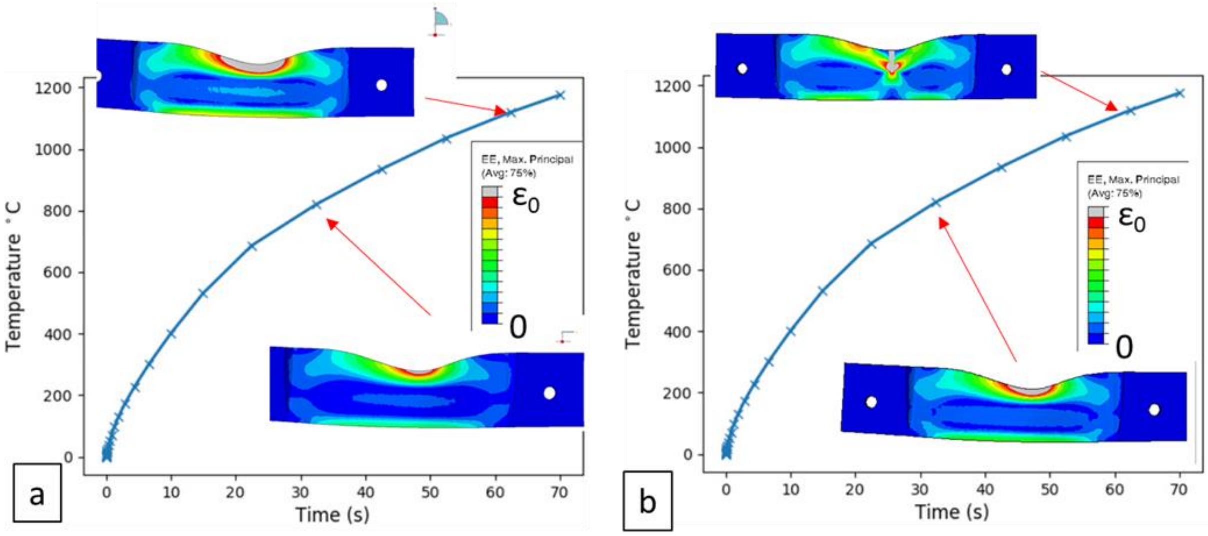

Figure 8: Evolution of the principal max strain field during the monotonic thermal loading (the curve corresponds to the temperature at the laser spot): (a) with the elastic behavior and (b) with the damage model ODM.

4.2 Modeling of the CMC/EBC behavior material under thermal gradient

In this part, the environmental barrier coating was modeled using shell elements and an elastic behavior with an elastic modulus of 90GPa, as indicated in [8]. The aim of this study was to assess the influence of the coating behavior on the damage kinematics of the specimen. As shown on Fig. 9, when the maximum temperature attains 800°C, the principal max strain overcomes the elastic threshold as previously when the CMC material was only considered (Fig. 8b). For this temperature, the strain level for the EBC material is lower than the elastic threshold. Thus, the damage scenario becomes by the matrix damage of the CMC. Then, with the temperature increases from 800°C to 1250°C, the principal max strain levels overcome the elastic threshold on both CMC and EBC materials. However, contrary to the previous study, the shape of the principal max strain field does not change for the CMC material. Indeed, the damaged area (in grey) seems to be similar to the one obtained with the model considering the CMC with an elastic behavior (Fig. 8a). This observation can be explained by the strength of the EBC layer, but also by the thickness ratio close to 1 between both materials, which prevent the yarn failure and the load transfer.

This result appears as a contradiction with the observation of the experimental critical failure.

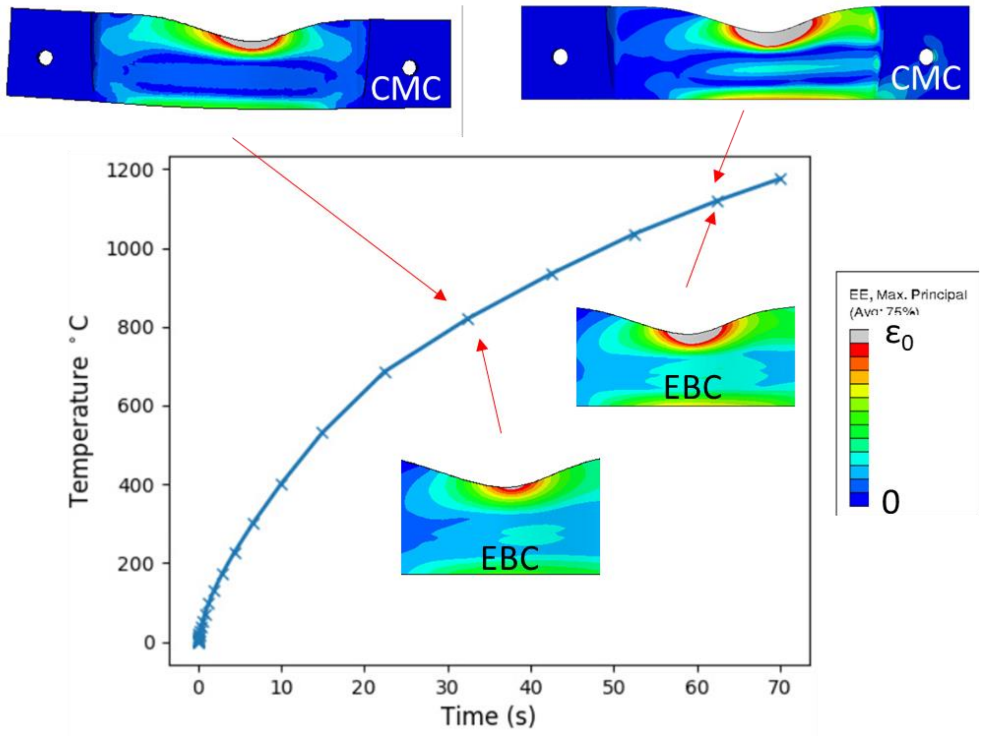

Figure 9: Evolution of the principal max strain field of the CMC and the EBC material during the monotonic thermal loading (the curve corresponds to the temperature at the laser spot)

9 CONCLUSIONS

The behavior of a CMC/EBC system under thermal gradient loadings was study in this work using three key points :

- the experimental characterization using a multi-instrumented high heat flux CO_2 laser setup
- the establishment of a finite element model ensuring a good correlation between experimental and numerical thermal fields
- the modeling of the behavior using on one hand the damage model ODM for the CMC substrate, and on the other hand the ODM model for the CMC and an elastic behavior for the EBC.

The main result is that the damage behavior of the CMC material must be taken into account to predict the behavior and the failure of the CMC/EBC specimen under thermal gradient loadings. Moreover, the localization of the yarn failure is correctly predicted.

Nevertheless, add the EBC layer, with an elastic behavior, in the finite element model strongly modifies the numerical prediction. Indeed, the critical failure of the specimen does not activate anymore due to the good strength of the top coat. This result indicates that a damage model for the EBC is also needed. This kind of model will be introduce in the future works.

ACKNOWLEDGEMENTS

This work was supported under ATLAAS, French research project co-funded by DGAC, ONERA and SAFRAN Group, involving SAFRAN Group, ONERA and CNRS.

REFERENCES

[1] J.A. Dever, M.V. Nathal and J.A. DiCarlo, Research on high-temperature aerospace materials at NASA Glenn Research Center, *Journal of Aerospace Engineering*, **26**, 2013, pp. 500–514 (doi: 10.1061/(ASCE)AS.1943-5525.0000321).

[2] E. Bouillon, Ceramic Matrix Composite behavior enhancement for Gas Turbines Hot Sections, *Conference of NATO Science and Technology Organization, AVT-356 Research Symposium on Physics of Failure for Military Platform Critical Subsystems, 2021*

[3] P.J. Meschter, E.J. Opila, and N.S. Jacobson, Water vapor–mediated volatilization of high-temperature materials, *Annual Review of Materials Research*, **43**, 2013, pp. 559–588 (doi: 10.1146/annurev-matsci-071312-121636).

[4] K. Lee, D. Waters, G. Costa and B. Puleo, *Current EBC development and testing at NASA*, Technical Report, 2017.

[5] M.P. Appleby, D. Zhu and G.N. Morscher, Mechanical properties and real-time damage evaluations of environmental barrier coated SiC/SiC CMCs subjected to tensile loading under thermal gradients, *Surface & coatings technology*, **284**, 2015, pp. 318–326 (doi: 10.1016/j.surfcoat.2015.07.042).

[6] T. Archer, M. Berny, P. Beauchêne and F. Hild, Creep behavior identification of an environmental barrier coating using full-field measurements, *Journal of the European Ceramic Society*, **40**, 2020, pp. 5704–5718 (doi: 10.1016/j.jeurceramsoc.2020.06.009).

[7] F. Laurin, N. Tableau, M. Kaminski, Z. Aboura and F. Bouillon, Validation of the onera damage model through comparisons with multi-instrumented structural tests on interlock woven ceramic matrix composites, *Proceedings of the 16th European Conference on Composites Materials, ECCM16, Séville, Spain, 2014*

[8] B.T. Richards, K.A. Young, F. de Francqueville, S. Sehr, M.R. Begley and H.N.G. Wadley, Response of ytterbium disilicate–silicon environmental barrier coatings to thermal cycling in water vapor, *Acta Materialia*, **106**, 2016, pp. 1–14 (doi: 10.1016/j.actamat.2015.12.053).